CrossMark

Creatine transporter deficiency leads to increased whole body and cellular metabolism

Marla K. Perna[1,5] · Amanda N. Kokenge[1,5] · Keila N. Miles[1,5] · Kenea C. Udobi[1,5] ·
Joseph F. Clark[2] · Gail J. Pyne-Geithman[3] · Zaza Khuchua[4,5] · Matthew R. Skelton[1,5]

Abstract Creatine (Cr) is a guanidino compound required for rapid replenishment of ATP in cells with a high-energy demand. In humans, mutations in the Cr transporter (*CRT*;*SLC6A8*) prevent Cr entry into tissue and result in a significant intellectual impairment, epilepsy, and aphasia. The lack of Cr on both the whole body and cellular metabolism was evaluated in Crt knockout ($Crt^{-/y}$) mice, a high-fidelity model of human CRT deficiency. $Crt^{-/y}$ mice have reduced body mass and, however, show a twofold increase in body fat. There was increased energy expenditure in a home cage environment and during treadmill running in $Crt^{-/y}$ mice. Consistent with the increases in the whole-body metabolic function, $Crt^{-/y}$ mice show increased cellular metabolism as well. Mitochondrial respiration increased in skeletal muscle fibers and hippocampal lysates from $Crt^{-/y}$ mice. In addition, $Crt^{-/y}$ mice had increased citrate synthase activity, suggesting a higher number of mitochondria instead of an increase in mitochondrial activity. To determine if the increase in respiration was due to increased mitochondrial numbers, we measured oxygen consumption in an equal number of mitochondria from $Crt^{+/y}$ and $Crt^{-/y}$ mice. There were no changes in mitochondrial respiration when normalized to mitochondrial number, suggesting that the increase in respiration observed could be to higher mitochondrial content in $Crt^{-/y}$ mice.

Keywords Creatine · Mitochondria · Creatine transporter · Creatine transporter deficiency

✉ Matthew R. Skelton
matthew.skelton@cchmc.org

1 Division of Neurology, Cincinnati Children's Research Foundation, 3333 Burnet Ave, ML 7044, Cincinnati, OH 45229, USA

2 Department of Neurology, University of Cincinnati College of Medicine, Cincinnati, USA

3 Department of Neurosurgery, University of Cincinnati College of Medicine, Cincinnati, USA

4 Heart Institute, Cincinnati Children's Research Foundation, Cincinnati, USA

5 Department of Pediatrics, University of Cincinnati College of Medicine, Cincinnati, USA

Introduction

The creatine transporter (CrT; *SLC6A8*) is a member of the solute carrier six family of sodium- and chloride-dependent transporters and is required for cellular uptake of creatine (Cr). Mutations in the CrT lead to Creatine Transporter Deficiency (CTD), which is characterized by moderate to severe intellectual disability, aphasia, and controllable epilepsy (deGrauw et al. 2003; DeGrauw et al. 2002). *SLC6A8* is located on the X-chromosome with CTD showing an X-linked pattern of inheritance (Gregor et al. 1995; deGrauw et al. 2003). CTD is a leading cause of X-linked intellectual disability (XLID), responsible for 1–3 % of all XLID (Rosenberg et al. 2004; Clark et al. 2006). To date, no treatment is available for CTD.

There are three known types of Cr deficiency syndromes (CDS) characterized by diminished Cr levels in the brain and periphery, and, additionally, decreased bioavailability of ATP to maintain normal cellular function. Cr deficiency syndromes (CDS) are a result of errors of Cr biosynthesis (AGAT and GAMT deficiency) or a global lack of Cr transporter (CTD) (Alcaide et al. 2011; Braissant et al. 2011; Schulze 2003; Stockler et al. 2007). Regardless of origin, CDS leads to severe developmental delay, epilepsy, and an

overall diminished quality of life. Oral Cr supplementation has been shown to ameliorate motor deficits in CDS resulting from defective biosynthesis (Morris et al. 2007); however, Cr supplementation has been ineffective in the treatment of CTD (van de Kamp et al. 2012). Of specific interest to the current study is the latter form of CDS, and in particular how a lack of CrT affects the overall metabolic function.

The primary role of creatine (Cr) is buffering ATP levels in high-energy tissues, such as brain and muscle. Cr kinase (CK) phosphorylates Cr to form readily available phosphate pools. Upon consumption of ATP, CK takes the phosphate group from phosphor-Cr and donates it to ADP. It has been estimated that in many high-energy cells, the majority of ATP generated by the mitochondria is used to make P-Cr that then diffuses into the cytoplasm (Wallimann et al. 2011). Acute loss of Cr using pharmacological agents that block the CrT in the heart leads to mitochondrial impairment and, ultimately, insufficient ATP to carry out normal cellular processes, suggesting perturbed energy metabolism in CTD (O'Gorman et al. 1996). Interestingly, GPA administration increased mitochondrial density in the striatum of mice (Horvath et al. 2011).

Evidence of mitochondrial dysfunction in other models of Cr deficiency suggests that mitochondrial function may also be abnormal in CTD. Neurons lacking creatine kinase have increased mitochondrial motility as compared to normal neurons (Kuiper et al. 2008). While the overall mitochondrial number was similar in CK-deficient neurons, there was an increase in motile mitochondria compared with neurons from wild-type animals. In an attempt to replenish ATP to areas with high-energy demands, CK-deficient cells may need to distribute mitochondria differently than normal cells. This increase in motility may reflect a compensatory response to energy shortages in CK-deficient neurons. In addition, in a mouse model of deficient Cr biosynthesis, an increased ATP synthase activity in brain and muscle points to adaptive mechanisms in response to ATP shortages (Schmidt et al. 2004), further supporting a role for metabolic dysfunction in CDS.

To better understand and to develop treatments for CTD, we have developed the CrT knockout ($Crt^{-/y}$) mouse that shows significant impairments in a battery of cognitive tests, suggesting that this mouse is a high-fidelity model of CTD (Skelton et al. 2011). The purpose of this study was to characterize the metabolic phenotype of $Crt^{-/y}$ mice by examining the whole-body metabolism, ATP levels, and mitochondrial respiration.

Methods

Subjects

$Crt^{+/y}$ and $Crt^{-/y}$ mice were derived from breeding CrT$^{+/-}$ females to $Crt^{+/y}$ males (Skelton et al. 2011). To control for litter effects, each experiment only used one $Crt^{+/y}$ and $Crt^{-/y}$ mouse from each litter. Mice were kept on a 14:10 light:dark cycle in the CCRF vivarium which is fully accredited by AAALAC and all experiments were approved by CCRF IACUC prior to the beginning of the experiment.

Whole-body calorimetry

Calorimetry was performed using the Oxymax system from Columbus Instruments (Columbus, OH) as previously described (Powers et al. 2013). Calorimetry was evaluated for 9 h during the initial light phase, 10 h for the dark phase, and 4 h during the morning light phase. Resting oxygen consumption and carbon dioxide production rates (VO_2 and VCO_2, respectively) were measured every 10 min and normalized to body weight. Animals were given free access to water and food during testing. Food was weighed following testing. A total of 8 $Crt^{+/y}$ and 10 $Crt^{-/y}$ mice were used.

The following day, mice were exercised on a motorized treadmill placed inside a sealed chamber. The initial speed of the treadmill was 5 m/min and was increased stepwise by 5 m/min every 5 min until a final speed of 25 m/min was reached. VO_2 and VCO_2 were sampled every 30 s and normalized to the body weight of the animal. Respiratory exchange ratio (RER), a measure that determines if carbohydrates, fatty acids, or protein are being utilized for energy (Simonson and DeFronzo 1990), and energy expenditure were calculated using the CLAX software from Columbus Instruments.

Body composition analysis

Body composition was determined using EchoMRI (Houston, TX). Briefly, animals were placed into the EchoMRI and total body fat, lean body mass, and water content that were derived for each animal. Body fat percentage was calculated by dividing body fat by mass.

ATP assay

$Crt^{+/y}$ and $Crt^{-/y}$ mice were decapitated following brief isofluorane anesthesia. The brain, heart, and gastrocnemius muscle were dissected and rapidly frozen in dry ice-cooled isopentane. Samples were weighed and homogenized in an equal volume of perchloric acid. ATP levels were analyzed using a commercially available fluorescence kit (Abcam Cambridge, MA). ATP levels were normalized to tissue weight. Percent control levels were determined by dividing all samples by the mean of the $Crt^{+/y}$ mice for the specific tissue studied.

High-resolution respirometry

Mitochondrial respiration was analyzed using the Oroboros Oxygraph-2K (Oroboros Instruments, Innsbruck, Austria).

Muscle fibers from the quadriceps and hippocampal lysates from $Crt^{+/y}$ and $Crt^{-/y}$ mice were prepared in MiR05 buffer (Gnaiger et al. 2000). Approximately 2 mg of wet-weight tissue was used in each preparation. Samples from $Crt^{+/y}$ and $Crt^{-/y}$ mice were run in the side-by-side chambers to minimize any ambient effects on mitochondrial respiration. Oxygen consumption and oxygen flux were monitored in real time using the DatLab4.3 software from Oroboros.

For hippocampal lysates, a substrate/uncoupler/inhibitor titration (SUIT) protocol was performed to assess mitochondrial respiration (Karlsson et al. 2013). Tissue was allowed to stabilize for approximately 15 min prior to the addition of substrates. Malate (5 mM) and pyruvate (5 mM) were added followed by ADP (1 mM) and glutamate (5 mM) to assess the NADH-related oxidative phosphorylation (OXPHOS) capacity of CI (OXPHOS CI). Maximal OXPHOS was stimulated by the addition of 10 mM succinate (OXPHOS CI + CII). Oligomycin was added to determine mitochondrial respiration independent of ATP production (LEAK CI + CII). A titration of carbonyl cyanide p-(trifluoromethoxy) phenylhydrazone (FCCP) was added until no further increase in OXPHOS capacity was observed (ETC CI + CII). Rotenone was added to assess ETC capacity through CII (ETC CII). Antimycin-A was added to inhibit electron flow through the ETC. Control ratios for OXPHOS CI + CII and ETC CI + CII were derived by dividing the respective rates by the LEAK respiration rate. Data were normalized to total protein levels as determined by the Bradford protein assay.

Muscle fibers were excised from $Crt^{+/y}$ and $Crt^{-/y}$ mice, permeabilized with 50 µg/ml of saponin, and placed into the Oxygraph in a similar manner as the hippocampi. To assess OXPHOS CI, 2.5 mM ADP and 5 mM glutamate were added sequentially. OXPHOS CI + CII was assessed by adding succinate and 5 mM ADP followed by the addition of cytochrome c (CytC) to assess the integrity of the outer membrane of the mitochondria. ETS CI + CII was determined using FCCP, and rotenone was added to evaluate ETS CII. Data were normalized to the wet weight of the fibers.

Seahorse XF24 assay

To assess the individual contribution of Complex I and Complex II in the respiratory increases in $Crt^{-/y}$ mice, mitochondrial function was assessed using equivalent amounts of mitochondrial protein in a Seahorse XF24e analyzer. Hippocampi from $Crt^{+/y}$ and $Crt^{-/y}$ mice ($n = 4$) were dissected on ice and homogenized in mitochondrial isolation buffer (320 mM sucrose, 10 mM Tris, 1 mM K^+ EDTA, and 2.5 g/l BSA, pH = 7.4) using a Teflon-glass homogenizer. Samples were centrifuged for 10 min at 1000 g to remove cellular debris. The lysate was collected and

centrifuged for 10 min at 6400 g. The lysate was removed, and the pellet containing the crude mitochondrial preparation was resuspended in mitochondrial activation solution (MAS) without BSA (70 mM sucrose, 210 mM mannitol, and 1 mM EGTA, pH 7.2). An aliquot was removed from the sample for protein level determination, and BSA was added to the remaining sample for a final concentration of 0.5 % (w/V). Mitochondria were kept on ice, while protein levels were determined using a Bradford assay according to the manufacturers suggestion. Samples were adjusted for mitochondrial protein levels, and 10 µg of mitochondrial protein in 50 µl of MAS solution from each subject was loaded onto the XF24 plate. The plate was centrifuged for 20 min at 2000 g using a swinging bucket rotor. The total volume in each well was then raised to 500 µl by adding warmed (37°) MAS solution containing either (a) malate (2 mM) and pyruvate (10 mM) or (b) rotenone (2 µM) and succinate (10 mM). The plate was then transferred to the XF24 analyzer, and the experiment was initiated. The XF24 samples oxygen consumption every 10 min and compounds were injected from the pre-loaded ports every 30 min. Injections were as follows (final concentration): (A) ADP (4 mM); (B) Oligiomycin (2.5 µg/mL); (C) FCCP (4 µM); and (D) antimycin-A (4 µM). Following the completion of the assay, protein levels were re-determined by Bradford assay and the data were normalized to protein levels. Samples were run in duplicate for each combination of sample and substrate.

Western blotting

Mitochondria from the hippocampus of $Crt^{-/y}$ and $Crt^{+/y}$ mice were isolated as described above and separated on 12 % Mini-PROTEAN® TGX pre-cast gels. Proteins were transferred to PVDF membranes and blocked using Odyssey blocking buffer (Li-Cor, Lincoln, Nebraska). Membranes were incubated with a Total OXPHOS Rodent WB Antibody Cocktail (Abcam, Cambridge, MA) at a 1:1000 dilution for 18 h at 4 °C. This cocktail contains five antibodies, each directed at a specific protein in the OXPHOS complex. Complex 1 is probed using NDUF88, Complex II is represented by SDHB, Complex III by UQCRC2, Complex IV by MTCO1, and Complex V by ATP5A. The blot was concurrently probed with an Actin antibody (Abcam) at a concentration of 1:500 as a loading control. Following washing of the primary antibody, the blot was incubated with 1:10,000 dilution of IRDye 680RD Donkey anti-mouse secondary antibody (Li-Cor, Lincoln Nebraska) for the OXPHOS proteins and a IRDye 800CW Donkey anti-goat antibody for actin (Li-Cor). Fluorescent images were acquired on an Odyssey CLx (Li-Cor) imager, and fluorescence was quantified using the software from the manufacturer. OXPHOS signals were normalized to the actin signal.

Statistical analysis

Mitochondrial respiration and whole-body calorimetry data were analyzed using two-way repeated measures ANOVA with gene and time as factors (Graphpad Prism, La Jolla, CA). Significant interactions were examined using Sidak correction, and data were considered significant if $p < 0.05$. ATP, weight, food consumption, and body composition were analyzed by two-tailed t test. Data are presented as mean ± SEM.

Results

Body composition

In agreement with the previous data, $Crt^{-/y}$ mice weighed less than their $Crt^{+/y}$ counterparts did ($t_{10} = 21.7$, $p < 0.001$; Fig. 1a). Body composition analysis showed that $Crt^{-/y}$ mice have an increase in body fat percentage when compared with $Crt^{+/y}$ mice ($t_{10} = 2.23$, $p < 0.05$; Fig. 1b). Over 23 h, $Crt^{-/y}$ mice consumed less food than $Crt^{+/y}$ mice ($t_{10} = 3.90$, $p < 0.05$; Fig. 1c); however, no differences were observed when adjusted for the body weight of the animal.

ATP levels

CrT$^{-/y}$ mice showed ATP reductions in the brain ($t_{10} = 2.3$, $p < 0.05$), heart ($t_{10} = 2.91$, $p < 0.05$), and gastrocnemius muscle ($t_9 = 6.7$, $p < 0.001$) compared with CrT$^{+/y}$ mice (Fig. 2).
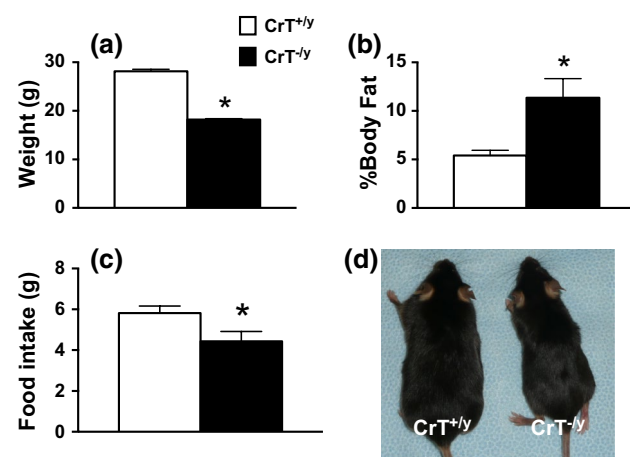

Fig. 1 $Crt^{-/y}$ mice show reductions in body weight (**a**) and food intake (**c**) compared with $Crt^{+/y}$ mice. Interestingly, $Crt^{-/y}$ mice had a higher body fat percentage (**b**) compared with $Crt^{+/y}$ mice. **d** Representative image of $Crt^{+/y}$ (*left*) and $Crt^{-/y}$ (*right*) mice. Values are mean ± SEM. *$p < 0.05$; $n = 6$–13 per group
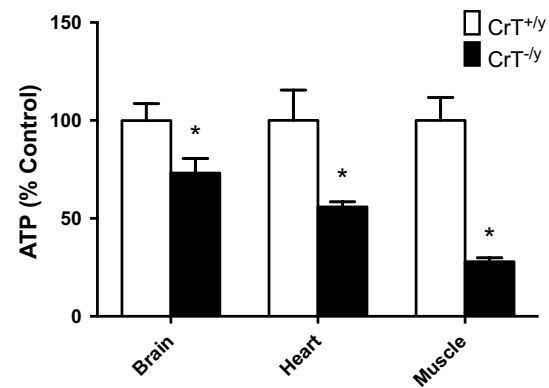
Fig. 2 $Crt^{-/y}$ mice have reduced ATP levels in the brain, heart, and muscle compared with $Crt^{+/y}$ mice. Values are mean ± SEM. *$p < 0.05$; $n = 6$ per group

Whole-body calorimetry-home cage

$Crt^{-/y}$ mice had increased oxygen consumption (VO_2) (gene: (F(1,16) = 18.6, $p < 0.001$; Fig. 3a) at rest compared with $Crt^{+/y}$ mice. Interactions between time and gene were observed; however, there were no consistent differences between individual time points. $Crt^{-/y}$ mice had increased CO_2 production (F(1,16) = 16.91, $p < 0.001$; Fig. 3b) compared with $Crt^{+/y}$ mice. When looking at energy expenditure, $Crt^{-/y}$ mice consumed more calories per body weight when compared with $Crt^{+/y}$ mice (F(1,16) = 17.32, $p < 0.001$; Fig. 3c). No significant difference in RER was observed (Fig. 3d).

Whole-body calorimetry-forced exercise

During treadmill running, $Crt^{-/y}$ mice consumed more oxygen (F(1,10) = 7.74, $p < 0.05$), produced more CO_2 (F(1,10) = 8.79, $p < 0.05$), and utilized more energy (F(1,10) = 8.16, $p < 0.05$) compared with $Crt^{+/y}$ mice (Fig. 4). There were no differences in RER.

Mitochondrial function

Increased mitochondrial respiration was observed in the hippocampus of $Crt^{-/y}$ mice compared with $Crt^{+/y}$ (main effect of gene: F(1,11) = 290.4; $p < 0.001$; Fig. 5a). A gene by substrate interaction was also observed (F(5,55) = 1601, $p < 0.001$). Increased respiration in response to stimulation of OXPHOS CI, OXPHOS CI + CII, LEAK CI + CII, ETC CI + CII, and ETC CII was observed in $Crt^{-/y}$ mice compared with controls ($p < 0.001$ for all measures). Respiratory control ratios for OXPHOS and the ETC were calculated based on this data with $Crt^{-/y}$ mice showing decreases in both measures ($p < 0.001$ for each measure; Fig. 5b).

Fig. 3 $Crt^{-/y}$ mice show increased oxygen consumpion (**a**) and carbon dioxide release (**b**) compared with $Crt^{+/y}$. $Crt^{-/y}$ mice also burned more calories than $Crt^{+/y}$ mice (**c**) while no changes were observed in RER (**d**). Line above x-axis denotes dark cycle of testing. $N = 8$–10 per group. Values are mean ± SEM
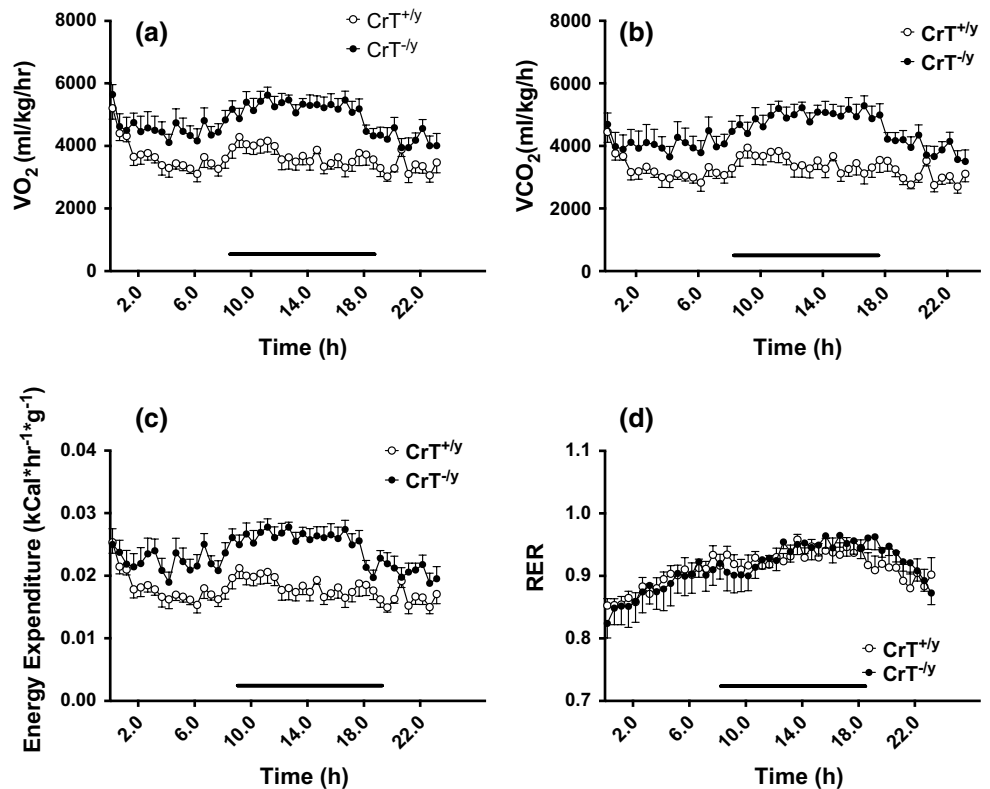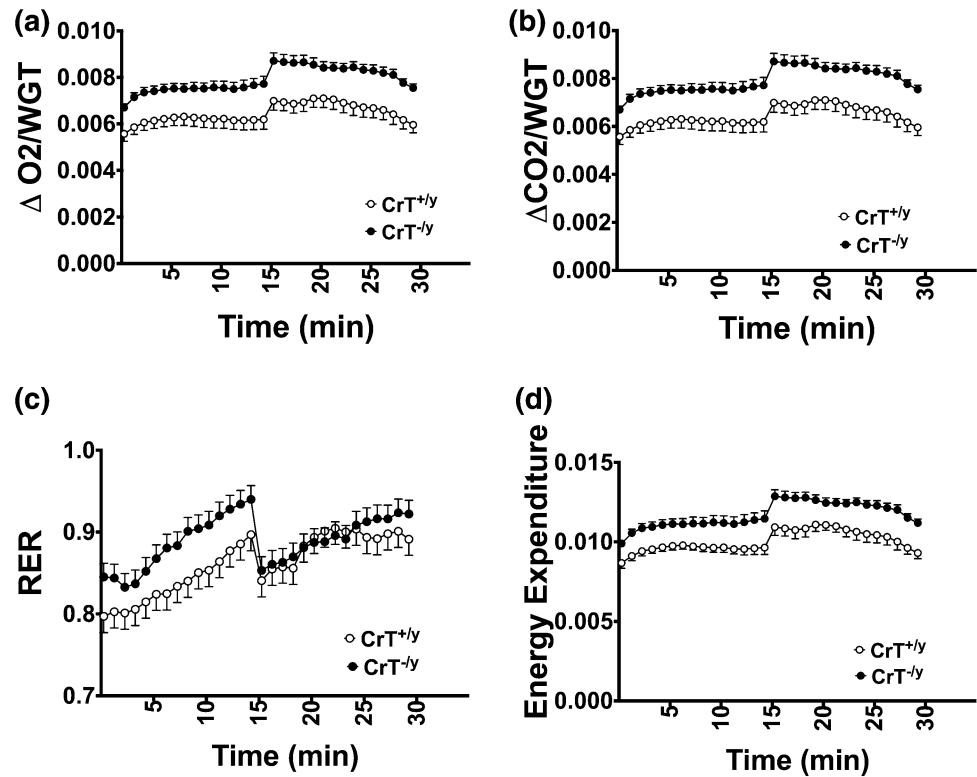

Fig. 4 $Crt^{-/y}$ mice show oxygen consupmtion (**a**), carbon dioxide release (**b**), and calorie use (**c**) compared with $Crt^{+/y}$ mice when exercising on a treadmill. As time progressed, speed was increased. The increase in gas exchange observed at ~15 min likely reflects a switch to alternate fuel sources. *$p < 0.05$; $n = 4$–6 per group. Values are mean ± SEM

Similar to the hippocampus, an overall increase in respiration was observed in the muscle of $Crt^{-/y}$ mice ($F(1,32) = 394.9$; $p < 0.001$; Fig. 5c). Increased oxygen consumption was observed following administration of all compounds except FCCP ($p < 0.01$ for all measures).
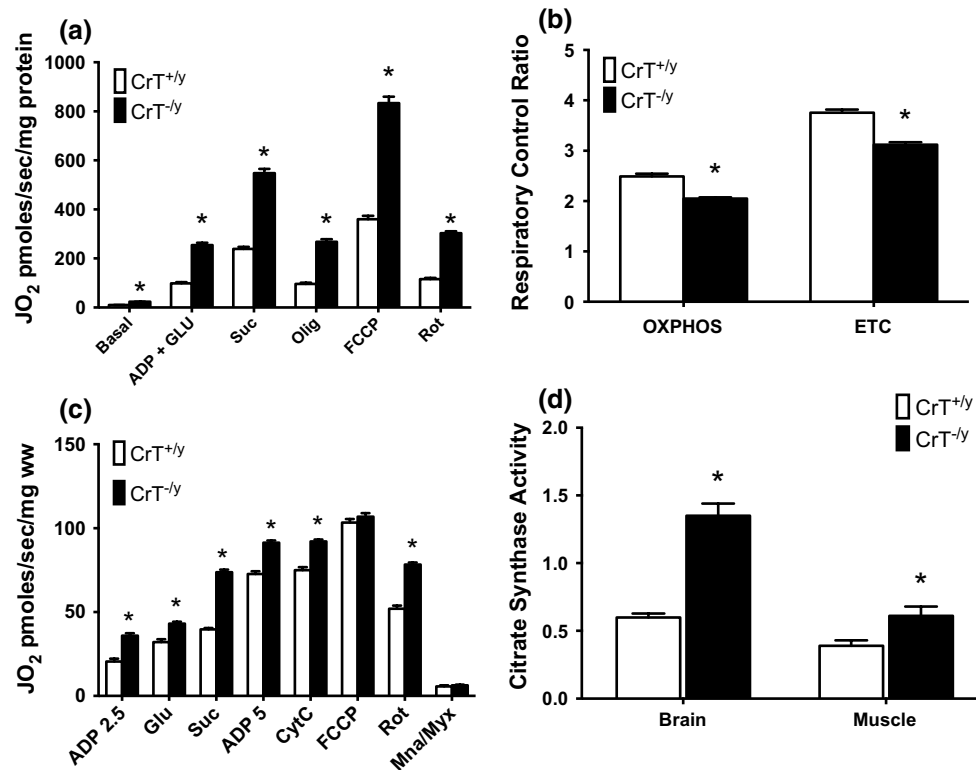
Fig. 5 $Crt^{-/y}$ mice show increased mitochondrial respiration (a) and respiratory control ratio (b) in hippocampal lysates. c Stimulated respiration was increased in permeabilized muscle fibers from $Crt^{-/y}$ mice. d Increased citrate synthase activity in samples tested for respirometry is observed in $Crt^{-/y}$ mice. *$p < 0.05$ $n = 6$ per group. Values are mean ± SEM

Citrate synthase activity was increased in all tissue regions examined ($p < 0.05$; Fig. 5d). The increase in CS activity is indicative of increased mitochondria. To determine if the changes observed were due to increases in mitochondrial number, equal amounts of mitochondria from the hippocampus of $Crt^{+/y}$ and $Crt^{-/y}$ mice were analyzed using the Seahorse XF24e. To elucidate possible mechanisms, a subset of mitochondria was given malate and pyruvate as substrates, while a second subset was provided with rotenone and succinate to assess complex I function. Oxygen consumption was evaluated following serial administration of ADP, oligomycin, FCCP, and antimycin-A. No changes in oxygen consumption were observed between genotypes (Fig. 6).

No differences were observed in relative levels of representative Complex I–Complex V proteins when examined by Western blotting (Fig. 7).

Discussion

It has been proposed that the Cr:P-Cr shuttle is the primary mechanism in which mitochondria-derived ATP is transported and utilized at cellular sites of high-energy demand

(Wallimann et al. 2011). In addition, it is thought that Cr is important for compartmentalizing changes in ATP:ADP ratios that could lead to changes in mitochondrial output. In this study, we show that the loss of Cr in mice via deletion of the CrT leads to an overall increase in mitochondrial respiration in the brain and muscle as well as reduced ATP levels. Increased CS activity suggests that the changes in mitochondrial respiration could be due to increased mitochondria in $Crt^{-/y}$ mice. When controlled for mitochondrial number, there are no differences in oxygen consumption between $Crt^{+/y}$ and $Crt^{-/y}$ mice. There were no changes in mitochondrial subunit protein levels when adjusted for the total mitochondrial protein level, further supporting the hypothesis that $Crt^{-/y}$ mice have more mitochondria than $Crt^{+/y}$ mice. Finally, $Crt^{-/y}$ mice show increased whole-body respiration and calorie consumption, again suggesting an increase in metabolism to compensate for a lack of the Cr-P-Cr buffer. Taken together, it appears that the loss of Cr leads to an increase in metabolic function.

$Crt^{-/y}$ mice have reduced ATP content and increased mitochondrial respiration: to our knowledge, this is the first study that comprehensively evaluates mitochondrial respiration in the brain of Cr-deficient animals. Cr stimulates mitochondrial respiration in the presence and
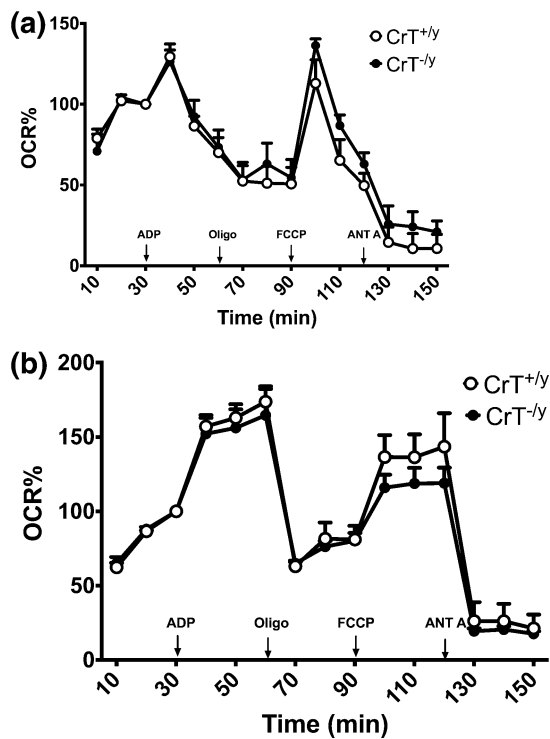
Fig. 6 Isolated mitochondria from the hippocampus of $Cr^{+/y}$ and $Crt^{-/y}$ mice show similar oxygen consumption when equal numbers of mitochondria are examined. **a** Oxygen consumption was examined in isolated mitochondria the presence of malate and pyruvate. No differences were observed between groups. **b** Complex II activity was assessed by incubating mitochondria with rotenone and succinate prior to respirometry. Values are mean ± SEM, $n = 4$, with each sample run in duplicate

Fig. 7 In isolated mitochondria from the hippocampus, no differences were observed in ETC CI through CV protein levels. Data were normalized to β-Actin and expressed as a percentage of $Crt^{+/y}$ control. $*p < 0.05$; $n = 4$ per group

absence of adenosine compounds (Saks et al. 2007). The data presented here are in agreement with studies that have depleted Cr using the Crt antagonist ß-guanidinopropionic acid (BPA; for meta-analysis, see Oudman et al. 2013). In this meta-analysis, chronic BPA administration reduces muscle Cr levels by 66 % and ATP levels by 39 %. Mitochondrial enzyme activity is elevated in the muscle, suggesting increased OXPHOS or increased mitochondrial content, consistent with our findings. In the brain, chronic GPA administration leads to a 26 % reduction in Cr and a 25 % reduction in ATP. An increase in mitochondrial markers was observed, again suggesting that there is an increase in mitochondria in the brain of Cr-depleted animals. The authors posited that there is a shift towards oxidative phosphorylation in GPA fed animals; our findings are consistent with this hypothesis.

Of the genetic Cr-deficient models, the CK-deficient mice are the most extensively studied (Kay et al. 2000). Similar to the $Crt^{-/y}$ mice, mice deficient in both isoforms of CK showed non-significant reductions in stimula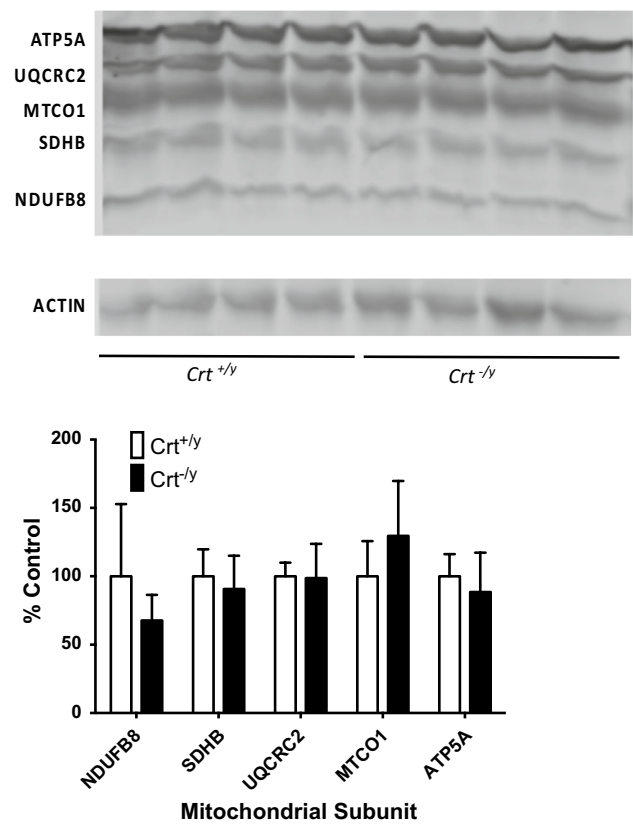ted respiration in cardiac fibers while showing increased respiration in muscle fibers (ter Veld et al. 2005). Mice deficient in the Cr-synthesizing enzyme arginine:gylcine amidinotransferase ($AGAT^{-/-}$) shows increased mitochondrial enzyme activity in the muscle. Citrate synthase activity is increased in the $AGAT^{-/-}$ mice as well (Nabuurs et al. 2013). The increase in mitochondrial activity and citrate synthase supports the findings in this study that Cr deficiency increases the number of mitochondria. The mitochondrial increases in Cr-deficient muscle likely compensates for reduced ATP or disrupted ATP:ADP or AMP:ATP ratios in the tissue. $Crt^{-/y}$ mice show significant reductions in ATP both in this study and as shown previously (Russell et al. 2014). AGAT-deficient mice have reduced muscular ATP (Nabuurs et al. 2013). CK knockout mice have ATP reductions during seizures and hypoxia (Kekelidze et al. 2001); paradoxically double CK knockout ($CK^{-/-}$) mice do not have ATP reductions (in 't Zandt et al. 2004). The discrepancy in ATP levels between the $CK^{-/-}$ and $Crt^{-/y}$ mice could provide valuable information on the mechanisms underlying the learning deficits observed in both models (Skelton et al. 2011; Streijger et al. 2005). In

addition, future studies on the maintenance of ATP levels CK-deficient mice could prove interesting.

$Crt^{-/y}$ mice show increased calorie consumption: $Crt^{-/y}$ mice have increased oxygen and CO_2 consumption at rest as well as during exercise. This further supports the hypothesis that $Crt^{-/y}$ mice increase metabolic output to compensate for the loss of tissue Cr. As $Crt^{-/y}$ mice do not appear to be hyperactive (Skelton et al. 2011), it is unlikely that the increases in gas exchange are due to increased activity by the $Crt^{-/y}$ mice. Cr is important in thermoregulation (Kazak et al. 2015), and it is possible that this plays a role in the metabolic increases seen in $Crt^{-/y}$ mice. Future studies will be designed to investigate the ability of the $Crt^{-/y}$ mouse to maintain body temperature in response to cold stress. Interestingly, there were no overall changes in RER which is known to correlate to the type of fuel (carbohydrate, fat or protein) being used for energy (Simonson and DeFronzo 1990). This suggests that $Crt^{-/y}$ mice do not differentially switch to alternate fuel sources when subjected to exercise.

$Crt^{-/y}$ mice have reduced stature and increased body fat: $Crt^{-/y}$ mice show reductions in body weight, similar to our previous study (Skelton et al. 2011). $Crt^{-/y}$ mice have increased body fat when compared with $Cr^{+/y}$ mice, suggesting that the weight differences seen are likely due to a loss in muscle mass. The reduction in lean body mass could be considered at odds with human data showing normal levels of Cr in the muscle of two CTD patients (Pyne-Geithman et al. 2004; deGrauw et al. 2003). There are now over 150 CTD patients; however, there have been no new reports on muscle Cr levels using either MRS or biochemical methods. Hypotonia is the second most common co-morbidity in CTD patients (Dunbar et al. 2014), suggesting that muscle is sensitive to the loss of Cr. A more comprehensive examination of muscle Cr levels in CTD patients is required prior to dismissing the muscle phenotype of $Crt^{-/y}$ mice as inconsistent with the human data.

In conclusion, CrT deficiency results in increased energy expenditure likely to compensate for reductions in ATP. The increased energy expenditure accompanies an increase in mitochondria in the muscle and brain of $Crt^{-/y}$ mice. The mechanism underlies these changes in currently unknown. Cr and CrT expressions have been linked to several metabolic signaling molecules, such as mTOR (Shojaiefard et al. 2006), PI3 kinase/AKT (Cunha et al. 2015), and AMP activated kinase (Nabuurs et al. 2013). Thus, studies to investigate the role of these kinases and signaling pathways in the CrT mediated changes in both mitochondrial function and the overall phenotype of these mice should be considered in future studies.

Compliance with ethical standards

Ethical statement All procedures involving animals have been approved by the Cincinnati Children's Research Foundation Institutional Animal Care and Use Committee (CCRF IACUC), which is fully accredited by the International Association for Assessment and Accreditation of Laboratory Animal Care.

Conflict of interest The authors declare no conflict of interest.

References

Alcaide P, Merinero B, Ruiz-Sala P, Richard E, Navarrete R, Arias A, Ribes A, Artuch R, Campistol J, Ugarte M, Rodriguez-Pombo P (2011) Defining the pathogenicity of creatine deficiency syndrome. Hum Mutat 32(3):282–291. doi:10.1002/humu.21421

Braissant O, Henry H, Beard E, Uldry J (2011) Creatine deficiency syndromes and the importance of creatine synthesis in the brain. Amino Acids 40(5):1315–1324. doi:10.1007/s00726-011-0852-z

Clark AJ, Rosenberg EH, Almeida LS, Wood TC, Jakobs C, Stevenson RE, Schwartz CE, Salomons GS (2006) X-linked creatine transporter (SLC6A8) mutations in about 1 % of males with mental retardation of unknown etiology. Hum Genet 119(6):604–610

Cunha MP, Budni J, Ludka FK, Pazini FL, Rosa JM, Oliveira A, Lopes MW, Tasca CI, Leal RB, Rodrigues AL (2015) Involvement of PI3K/Akt signaling pathway and its downstream intracellular targets in the antidepressant-like effect of creatine. Mol Neurobiol. doi:10.1007/s12035-015-9192-4

DeGrauw TJ, Salomons GS, Cecil KM, Chuck G, Newmeyer A, Schapiro MB, Jakobs C (2002) Congenital creatine transporter deficiency. Neuropediatrics 33(5):232–238

deGrauw TJ, Cecil KM, Byars AW, Salomons GS, Ball WS, Jakobs C (2003) The clinical syndrome of creatine transporter deficiency. Mol Cell Biochem 244(1–2):45–48

Dunbar M, Jaggumantri S, Sargent M, Stockler-Ipsiroglu S, van Karnebeek CD (2014) Treatment of X-linked creatine transporter (SLC6A8) deficiency: systematic review of the literature and three new cases. Mol Genet Metab 112(4):259–274. doi:10.1016/j.ymgme.2014.05.011

Gnaiger E, Kuznetov AV, Schneeberger S, Seiler R, Brandacher G, Steurer W, Margreiter R (2000) Mitochondria in the Cold. In: Helmaier G, Klingenspor M (eds) Life in the Cold. Springer, New York, pp 431–442

Gregor P, Nash SR, Caron MG, Seldin MF, Warren ST (1995) Assignment of the creatine transporter gene (SLC6A8) to human chromosome Xq28 telomeric to G6PD. Genomics 25(1):332–333

Horvath TL, Erion DM, Elsworth JD, Roth RH, Shulman GI, Andrews ZB (2011) GPA protects the nigrostriatal dopamine system by enhancing mitochondrial function. Neurobiol Dis 43(1):152–162. doi:10.1016/j.nbd.2011.03.005

in 't Zandt HJ, Renema WK, Streijger F, Jost C, Klomp DW, Oerlemans F, Van der Zee CE, Wieringa B, Heerschap A (2004) Cerebral creatine kinase deficiency influences metabolite levels and morphology in the mouse brain: a quantitative in vivo 1H and 31P magnetic resonance study. J Neurochem 90(6):1321–1330

Karlsson M, Hempel C, Sjovall F, Hansson MJ, Kurtzhals JA, Elmer E (2013) Brain mitochondrial function in a murine model of cerebral malaria and the therapeutic effects of rhEPO. Int J Biochem Cell Biol 45(1):151–155. doi:10.1016/j.biocel.2012.08.008

Kay L, Nicolay K, Wieringa B, Saks V, Wallimann T (2000) Direct evidence for the control of mitochondrial respiration by mitochondrial creatine kinase in oxidative muscle cells in situ. J Biol Chem 275(10):6937–6944

Kazak L, Chouchani ET, Jedrychowski MP, Erickson BK, Shinoda K, Cohen P, Vetrivelan R, Lu GZ, Laznik-Bogoslavski D, Hasenfuss SC, Kajimura S, Gygi SP, Spiegelman BM (2015) A creatine-driven substrate cycle enhances energy expenditure and thermogenesis in beige Fat. Cell 163(3):643–655. doi:10.1016/j.cell.2015.09.035

Kekelidze T, Khait I, Togliatti A, Benzecry JM, Wieringa B, Holtzman D (2001) Altered brain phosphocreatine and ATP regulation when mitochondrial creatine kinase is absent. J Neurosci Res 66(5):866–872

Kuiper JW, Oerlemans FT, Fransen JA, Wieringa B (2008) Creatine kinase B deficient neurons exhibit an increased fraction of motile mitochondria. BMC Neurosci 9:73. doi:10.1186/1471-2202-9-73

Morris AA, Appleton RE, Power B, Isherwood DM, Abernethy LJ, Taylor RW, Turnbull DM, Verhoeven NM, Salomons GS, Jakobs C (2007) Guanidinoacetate methyltransferase deficiency masquerading as a mitochondrial encephalopathy. J Inherit Metab Dis 30(1):100. doi:10.1007/s10545-006-0478-2

Nabuurs CI, Choe CU, Veltien A, Kan HE, van Loon LJ, Rodenburg RJ, Matschke J, Wieringa B, Kemp GJ, Isbrandt D, Heerschap A (2013) Disturbed energy metabolism and muscular dystrophy caused by pure creatine deficiency are reversible by creatine intake. J Physiol 591(Pt 2):571–592. doi:10.1113/jphysiol.2012.241760

O'Gorman E, Beutner G, Wallimann T, Brdiczka D (1996) Differential effects of creatine depletion on the regulation of enzyme activities and on creatine-stimulated mitochondrial respiration in skeletal muscle, heart, and brain. Biochim Biophys Acta 1276(2):161–170

Oudman I, Clark JF, Brewster LM (2013) The effect of the creatine analogue beta-guanidinopropionic acid on energy metabolism: a systematic review. PLoS One 8(1):e52879. doi:10.1371/journal.pone.0052879

Powers C, Huang Y, Strauss A, Khuchua Z (2013) Diminished exercise capacity and mitochondrial bc1 complex deficiency in tafazzin-knockdown mice. Front Physiol 4:74. doi:10.3389/fphys.2013.00074

Pyne-Geithman GJ, DeGrauw TJ, Cecil KM, Chuck G, Lyons MA, Ishida Y, Clark JF (2004) Presence of normal creatine in the muscle of a patient with a mutation in the creatine transporter: a case study. Mol Cell Biochem 262(1–2):35–39

Rosenberg EH, Almeida LS, Kleefstra T, deGrauw RS, Yntema HG, Bahi N, Moraine C, Ropers HH, Fryns JP, DeGrauw TJ, Jakobs C, Salomons GS (2004) High prevalence of SLC6A8 deficiency in X-linked mental retardation. Am J Hum Genet 75(1):97–105

Russell AP, Ghobrial L, Wright CR, Lamon S, Brown EL, Kon M, Skelton MR, Snow RJ (2014) Creatine transporter (SLC6A8) knockout mice display an increased capacity for in vitro creatine biosynthesis in skeletal muscle. Front Physiol 5:314. doi:10.3389/fphys.2014.00314

Saks V, Kaambre T, Guzun R, Anmann T, Sikk P, Schlattner U, Wallimann T, Aliev M, Vendelin M (2007) The creatine kinase phosphotransfer network: thermodynamic and kinetic considerations, the impact of the mitochondrial outer membrane and modelling approaches. Subcell Biochem 46:27–65

Schmidt A, Marescau B, Boehm EA, Renema WK, Peco R, Das A, Steinfeld R, Chan S, Wallis J, Davidoff M, Ullrich K, Waldschutz R, Heerschap A, De Deyn PP, Neubauer S, Isbrandt D (2004) Severely altered guanidino compound levels, disturbed body weight homeostasis and impaired fertility in a mouse model of guanidinoacetate N-methyltransferase (GAMT) deficiency. Hum Mol Genet 13(9):905–921. doi:10.1093/hmg/ddh112

Schulze A (2003) Creatine deficiency syndromes. Mol Cell Biochem 244(1–2):143–150

Shojaiefard M, Christie DL, Lang F (2006) Stimulation of the creatine transporter SLC6A8 by the protein kinase mTOR. Biochem Biophys Res Commun 341(4):945–949. doi:10.1016/j.bbrc.2006.01.055

Simonson DC, DeFronzo RA (1990) Indirect calorimetry: methodological and interpretative problems. Am J Physiol 258(3 Pt 1):E399–E412

Skelton MR, Schaefer TL, Graham DL, Degrauw TJ, Clark JF, Williams MT, Vorhees CV (2011) Creatine transporter (CrT; Slc6a8) knockout mice as a model of human CrT deficiency. PLoS One 6(1):e16187. doi:10.1371/journal.pone.0016187

Stockler S, Schutz PW, Salomons GS (2007) Cerebral creatine deficiency syndromes: clinical aspects, treatment and pathophysiology. Subcell Biochem 46:149–166

Streijger F, Oerlemans F, Ellenbroek BA, Jost CR, Wieringa B, Van der Zee CE (2005) Structural and behavioural consequences of double deficiency for creatine kinases BCK and UbCKmit. Behav Brain Res 157(2):219–234

ter Veld F, Jeneson JA, Nicolay K (2005) Mitochondrial affinity for ADP is twofold lower in creatine kinase knock-out muscles. Possible role in rescuing cellular energy homeostasis. FEBS J 272(4):956–965. doi:10.1111/j.1742-4658.2004.04529.x

van de Kamp JM, Pouwels PJ, Aarsen FK, ten Hoopen LW, Knol DL, de Klerk JB, de Coo IF, Huijmans JG, Jakobs C, van der Knaap MS, Salomons GS, Mancini GM (2012) Long-term follow-up and treatment in nine boys with X-linked creatine transporter defect. J Inherit Metab Dis 35(1):141–149. doi:10.1007/s10545-011-9345-1

Wallimann T, Tokarska-Schlattner M, Schlattner U (2011) The creatine kinase system and pleiotropic effects of creatine. Amino Acids 40(5):1271–1296